Progress In Electromagnetics Research, PIER 40, 271–294, 2003

PHYSICAL SPLINE FINITE ELEMENT (PSFEM) SOLUTIONS TO ONE DIMENSIONAL ELECTROMAGNETIC PROBLEMS

X. Zhou †

Department of Electrical Engineering
Arizona State University, AZ, USA

Abstract—In this paper, a new computational technique is presented for the first time. In this method, physical differential equations are incorporated into interpolations of basic element in finite element methods. This is named physical spline finite element method (PSFEM). Theoretically, the physical spline interpolation introduces many new features. First, physical equations can be used in the interpolations to make the interpolations problem-associated. The algorithm converges much faster than any general interpolation while keeping the simplicity of the first order Lagrange interpolation. Second, the concept of basis functions may need to be re-examined. Thirdly, basis functions could be complex without simple geometric explanations.

The applications to typical one-dimensional electromagnetic problems show the great improvements of the newly developed PSFEM on accuracy, convergence and stability. It can be extended to other applications. Extension to two- and three-dimensional problems is briefly discussed in the final section.

† The author is currently with Agere Systems Inc. His current mailing address is 156 Wyndham Drive, Allentown, PA, 18104, USA

1. INTRODUCTION

The finite element method (FEM) has become one of the most important and practical engineering tools for scientists and engineers. It has been used to solve mechanical problems [1, 2], electromagnetic problems [3–5], and many other mathematical and physical problems. Lots of applications in electromagnetic theory have been collected in [6]. New literature are appearing in many academic journals and conferences. Some commercial software based on FEM are important tools in industries. Many efforts have been paid to the efficiency, accuracy and flexibility of FEM from the mathematical point of view. Great progress has been made on the implementation of FEM since electronic computer was invented. In research, one of the trends is to incorporate more efficient mathematical solvers into FEM of large scale problems. The second trend is to construct better elements to make FEM more flexible in modeling complex structures. Adaptive technique is also used. The third trend is to use the so-called p-elements [7] and hp-elements [8] to improve accuracy and efficiency of FEM. Of course, like any other numerical methods, artificial boundary conditions (ABC) are always important for open problems. As we expected, applications could be extended without limitations.

In the theoretical aspects, the Rayleigh-Ritz's method and Galerkin's method are the most popular ones. Although not all problems can be dealt with the Rayleigh-Ritz's method, the Rayleigh-Ritz's method provides the foundations of the finite element method [4]. The Rayleigh-Ritz's method is based on the stationary characteristics of variational functionals that are related to minimum energy principle in mechanics. It was first introduced by Rayleigh

in 1877 and was extended after 30 years by Ritz in 1907. Once the formulation is obtained, interpolation choice is another important task. Up to now, Lagrange polynomials are the most popular choices. As pointed out by Noor [9, p. 26], trigonometric and exponential bases are not recommended since they generally have poor approximation properties for FEM computations. p (hp)-elements are too complicated and not always better than lower order approximations. A typical example is the well-known serpentine curve [10]. Recently, wavelet type basis functions are also adopted [11]. But the construction of good wavelets is not easy. In most cases, there are no closed forms. Although the final matrices are sparse, the time is spent on the construction of wavelets.

Another interpolation technique — spline — has been ignored for a long time because of the following reasons: (1) They are too difficult to implement in most two and three dimensional problems [12]. (2) Splines are too smooth to be applied to inhomogeneous problems [9, p. 26]. Special modifications must be used at the joints [13]. Then, applications of spline functions in solving differential (linear and nonlinear) and integral equations are mostly limited to theoretical investigations [14–16]. Very few applications in electrical engineering have been found [17]. Furthermore, only B-splines are practically used. Similar to wavelet basis functions, B-spline basis functions are not simple.

On the other hand, all the existing interpolations are inherently general mathematical tools. The expansions have nothing to do with the physical problems but pure mathematical expansions. Because of this property, they can be used anywhere in principle, but may not be efficient and accurate.

In this paper, a novel physical spline expansion is introduced. This idea is motivated by the following intuition: if we can incorporate the properties of the physical equations into the corresponding expansions, we can solve these physical problems much more efficiently and accurately. In this approach, some conventional concepts must be extended. For example, all existing basis functions are always chosen to be real. They have intuitive and geometric explanations [4, p. 421]. This limitation is not necessary and will be removed. According to the stationary property of a functional, the only requirement on the expansion is that the functional must be differentiable with respect to the expansion coefficients. If the coefficients are complex, the functional must be analytic with respect to the coefficients. According to complex analysis, Cauchy-Riemann (C-R) equations must be satisfied. C-R equations ensure that the stationary value can be reached from any direction on the complex plane. It is worth pointing

out that although the method used in [4, Appendix B] yields useful results, the procedure for complex-valued problems is not rigorous. Obviously, the procedure only ensures the stationary value along the real and imaginary axes.

The physical spline expansion presented in this paper is based on the well-known cubic spline interpolation that is used widely in data processing, curve fitting, computer graphics. However, traditional cubic spline is not convenient for FEM implementation. Incorporation of the differential equations changes the situation dramatically. The expansion theory will be presented in Sec. 3, application to FEM in the following sections. Several classical examples are solved to show the great improvement of the present method from theoretical and practical points of view.

In this paper, only one-dimensional (1D) problems are discussed to emphasize the idea, procedure and power of the method without being distracted by the complexity of two dimensional(2D) and three-dimensional(3D) problems. Although 1D problems themselves are not very useful in general and analytical solutions exist in most cases, numerical solutions are preferred in some applications [18]. They are also the best to illustrate a new technique. It is easier to have some theoretical observations on a new technique in 1D problems. Some 2D problems can be simplified to be 1D problems [4]. Extension to two- and three-dimensional problems is briefly discussed in the final section.

2. VARIATIONAL FORMULATION OF GENERAL 1D PROBLEMS

Almost all techniques are examined in one-dimensional (1D) problems first, and then are extended to higher dimensions. Most linear one-dimensional problems can be recognized as special cases of one-dimensional Sturm-Liouville differential equation [5]

$$-\frac{d}{dx}\left(p(x)\frac{dU}{dx}\right)+q(x)U(x)=f(x), \quad (0<x<x_a) \tag{1}$$

where $p(x)$ and $q(x)$ are knowns and $U(x)$ is the unknown. Several special interpretations are discussed in [5]. Now, for generality, we just treat (1) as a mathematical equation. Boundary conditions can be generalized as

$$U=Q_0, \ (x=0, \text{ or } x=x_a) \tag{2}$$

$$\frac{\partial U}{\partial x}+\alpha U=\beta, \ (x=0, \text{ or } x=x_a) \tag{3}$$

(2) is the essential boundary condition. (3) is the generalized impedance boundary conditions.

It is easy to get the functional expression by applying the principle of virtual power to (1)

$$\left\langle -\frac{d}{dx}\left(p(x)\frac{dU}{dx}\right) + q(x)U(x) - f(x), \delta U \right\rangle = 0$$

The functional is

$$\begin{aligned} F(u) \;=\; & \frac{1}{2}\int_0^{x_a}\left[p(x)\left(\frac{dU}{dx}\right)^2 + q(x)U^2(x)\right]dx \\ & - \int_0^{x_a} f(x)U(x)dx + p(x)\left[\frac{\alpha}{2}U^2 - \beta U\right]\Big|_0^{x_a} \end{aligned} \tag{4}$$

in which the boundary condition (3) is included. The essential boundary condition (2) must be forced if it holds.

3. PHYSICAL SPLINE EXPANSION AND ITS FINITE ELEMENT IMPLEMENTATION

Equation (1) claims that the second derivatives of U must be continuous in uniform regions, i.e., U belongs to the smoothness class $C^2[0,1]$. At an interface between different uniform regions, (1) holds on both sides. In electromagnetics, the interface condition is determined by Maxwell's equations. On one hand, (4) (plus essential boundary conditions if necessary) is not equivalent to the original problem (1) exactly if the derivatives are not considered properly. If the smoothness of U is lowered [15], the solution to (4) can still be obtained, but that is not exactly the solution to (1). On the other hand, most traditional interpolations in FEM do not satisfy the smoothness requirements at joints of elements in continuous regions in which $p(x)$, $q(x)$ and $f(x)$ are continuous. For example, the second order derivative of the first order Lagrange interpolations does not exist, even rational and algebraic elements etc. are discontinuous at joints of elements. Note that the so-called isoparametric elements do not change the properties of interpolations, they change the shapes of elements only. Furthermore, some of the existing interpolations are too smooth compared to what (1) requires within elements. Higher order Lagrange interpolations have higher (than second order) smooth derivatives that may not be required by (1). Strictly speaking, all the above drawbacks imply that the solutions may not be in $C^2[0,1]$, which may numerically lead to unpredictable bad approximations of the true solutions although

theoretically the functional converges to the space. These solutions are called weak solutions of (1) [4, 22].

Might we overcome the above shortcomings? They are physical drawbacks rather than just mathematical ones. Splines are tools designed for smoothing data. They may be the right choice. However, if we use splines in solving partial differential equations (PDE) directly, we will have some problems. (a) It makes the procedure too complicated; (b) Splines are too smooth at discontinuous interfaces such as the interfaces among different dielectrics; (c) They are still general. No information about the differential equation (1) is included. In fact, only B-splines are used [15, 19].

Cubic spline may be the best starting point since its first order derivatives are smooth and the second order derivatives are continuous. This property is good for uniform regions, but too much for discontinuous dielectrics. It is also not easy to implement. The flexible choice of end conditions is not desired either. However, its main property matches partly what we desire. Let us start from it to develop a completely new technique.

It is shown that there is only one way to construct cubic spline [20]. Within an element (x_1^e, x_2^e), it is

$$U^e(x) = \sum_{i=1}^{2} \left[N_i^e(x) U_i^e + M_i^e(x) (U_i^e)'' \right] \tag{5}$$

where

$$N_1^e(x) = \frac{x_2^e - x}{x_2^e - x_1^e} \tag{6a}$$

$$N_2^e(x) = \frac{x - x_1^e}{x_2^e - x_1^e} = 1 - N_1^e(x) \tag{6b}$$

$$M_1^e(x) = \frac{1}{6} \left[(N_1^e)^3 - N_1^e \right] (x_2^e - x_1^e)^2 \tag{6c}$$

$$M_2^e(x) = \frac{1}{6} \left[(N_2^e)^3 - N_2^e \right] (x_2^e - x_1^e)^2 \tag{6d}$$

Obviously, $0 \le |N_i^e| \le 1$, $M_i^e \le 0$. Although U may be complex, the real and imaginary parts satisfy the same conditions respect to space. Unfortunately, since the second order derivatives are usually unknown in general interpolation of data, there are algorithms based on the continuity of the first order derivatives for solving the second derivatives. Natural and Not-a-knot end conditions etc. are employed. In the natural cubic spline, the second order derivatives of the first and last nodes are set to be zero. In the Not-a-knot condition, the second

derivatives of the first and second nodes (knots) are forced to be equal. Similarly, for the last and last second nodes. Our application is quite different from pure data interpolation. The equation (1) governs the behavior of the function $U(x)$. In electromagnetics, $p(x)$ and $q(x)$ are associated with the characteristics of dielectrics. It is reasonable to make $p(x) = p^e$ and $q(x) = q^e$ constants within an element. Then (1) implies

$$(U_i^e)'' = -\frac{1}{p^e} f(x_i^e) + \frac{q^e}{p^e} U_i^e, \quad (i = 1, 2) \tag{7}$$

(5) becomes then

$$U^e(x) = \sum_{i=1}^{2} \left\{ \left[N_i^e(x) + \frac{q^e}{p^e} M_i^e(x) \right] U_i^e - \frac{1}{p^e} f(x_i^e) M_i^e(x) \right\} \tag{8}$$

Since (8) is a combination of cubic spline and physical equation, it is called physical spline (PS), and its corresponding FEM implementation will be called physical spline FEM (PSFEM). In (8), the second derivative U'' does not appear explicitly. The key is that the differential equation (1) is embedded successfully into the interpolation. It has to be noticed that the smoothness of the first order derivatives is guaranteed by the continuity of the second order derivatives according to functional theory. Therefore the continuity of the first order derivatives in not necessary to be forced if the second order derivatives are known. In traditional spline theory and applications, algorithms such as Thomas Algorithm [21] are developed to determine the unknown second order derivatives. The continuity of the first order derivatives is used (not "required") to construct the linear equations of the second order derivatives (Eq. (3.3.7) in [20]). Even though, the problem is still not complete since the end conditions are needed as described before. It is worthy of pointing out that the statement "However, we have not required that the first derivative, computed from equation (3.3.5), be continuous across the boundary between two intervals." is then not proper. In terms of U_i^e, U'' is known in our case, and (8) does not break the continuity of the second order derivatives in uniform spaces. So the algorithms required traditionally and the end conditions are completely avoided. The solution must belong to $C^2[0, 1]$ in uniform regions. The introduction of (7) makes the interpolation more physically reasonable. In uniform regions, the first order derivatives are smooth and the second order derivatives are continuous. At discontinuous interface, the second order derivatives satisfy the physical equations as expected. This may accelerate the convergence of the algorithm as we will see in the next sections. From the mathematical point of view, (7) relates U'' to U directly. It is

expected that (8) keeps the same simplicity of the first order Lagrange interpolation. We will make more comments on this technique in the numerical examples.

Since $\partial U_i^e/\partial U_i^e = 1$, even for complex-valued U_i^e, the stationary value of (4) can be achieved by using (8). Substituting

$$\begin{aligned} U &= \sum_{e=1}^{N_e} U^e \\ &= \sum_{e=1}^{N_e}\sum_{i=1}^{2}\left[B_i^e(x)U_i^e - \frac{1}{p^e}f(x_i^e)M_i^e(x)\right] \end{aligned} \tag{9}$$

where

$$B_i^e(x) = N_i^e(x) + \frac{q^e}{p^e}M_i^e(x) \tag{10}$$

into (4) and taking derivative with respect to the expansion coefficients, and following the regular procedure used in FEM [4, 5], we get

$$\begin{aligned} \sum_{e=1}^{N_e}\sum_{i=1}^{2}\int_0^{x_a}\Bigg\{ & p(x)\frac{dB_j^g}{dx}\frac{d}{dx}\left[B_i^e(x)U_i^e - \frac{1}{p^e}f(x_i^e)M_i^e(x)\right] \\ & + q(x)B_j^g\left[B_i^e(x)U_i^e - \frac{1}{p^e}f(x_i^e)M_i^e(x)\right]\Bigg\}dx \\ & - \int_0^{x_a} f(x)B_j^g(x)dx - p(x)B_j^g\frac{dU}{dx}\Big|_0^{x_a} = 0 \end{aligned} \tag{11}$$

Because $B_j^g(x)$ is localized within one element, $g = e$. Since at boundary points, $B_i^{1,N} = 1$, incorporation of the contributions of endpoints remains the same as in traditional FEM. The matrix from of (11) is

$$[A_{ij}^e][U_j^e] + [endpoints] = [b_i^e] + [{}_aA_{ij}^e][1] \tag{12}$$

where [*endpoints*] represents the contributions of boundaries. The traditional method [5] is used to enforce them. [1] is a $N \times 1$ vector.

$$A_{ij}^e = \int_{x_1^e}^{x_2^e}\left[p^e\frac{dB_i^e}{dx}\frac{dB_j^e}{dx} + q^eB_i^eB_j^e\right]dx \tag{13}$$

$$b_i^e = \int_{x_1^e}^{x_2^e} B_i^e(x)f(x)dx \tag{14}$$

$${}_aA_{ij}^e = f(x_j)\int_{x_1^e}^{x_2^e}\left[\frac{dB_i^e}{dx}\frac{dM_j^e}{dx} + \frac{q^e}{p^e}B_i^eM_j^e\right]dx \tag{15}$$

In the form of (12), $[A^e]$ and $[{}_aA^e]$ have the same assembly procedure. The following integrals can be used to simplify the computations of (13), (14) and (15).

$$\int_{x_1^e}^{x_2^e}(N_i^e)^2 = \frac{1}{3}h^e \tag{16a}$$

$$\int_{x_1^e}^{x_2^e}N_i^eN_j^e = \frac{1}{6}h^e, \quad (i\neq j) \tag{16b}$$

$$\int_{x_1^e}^{x_2^e}\left(\frac{dN_i^e}{dx}\right)^2 = \frac{1}{h^e} \tag{16c}$$

$$\int_{x_1^e}^{x_2^e}\left(\frac{dN_i^e}{dx}\right)\left(\frac{dN_j^e}{dx}\right) = -\frac{1}{h^e} \quad (i\neq j) \tag{16d}$$

$$\int_{x_1^e}^{x_2^e}(M_i^e)^2 = \frac{2}{945}(h^e)^5 \tag{16e}$$

$$\int_{x_1^e}^{x_2^e}M_i^eM_j^e = \frac{31}{15120}(h^e)^5, \quad (i\neq j) \tag{16f}$$

$$\int_{x_1^e}^{x_2^e}\left(\frac{dM_i^e}{dx}\right)^2 = \frac{1}{45}(h^e)^3 \tag{16g}$$

$$\int_{x_1^e}^{x_2^e}\left(\frac{dM_i^e}{dx}\right)\left(\frac{dM_j^e}{dx}\right) = \frac{7}{360}(h^e)^3, \quad (i\neq j) \tag{16h}$$

$$\int_{x_1^e}^{x_2^e}N_i^eM_j^e = -\frac{7}{360}(h^e)^3, \quad (i\neq j) \tag{16i}$$

$$\int_{x_1^e}^{x_2^e}N_i^eM_i^e = -\frac{1}{45}(h^e)^3 \tag{16j}$$

$$\int_{x_1^e}^{x_2^e}\left(\frac{dN_i^e}{dx}\right)\left(\frac{dM_j^e}{dx}\right) = 0, \quad (i,j=1,2) \tag{16k}$$

where $h^e = x_2^e - x_1^e$. Therefore

$$A_{11}^e = p^e\left[\frac{1}{h^e}+\frac{1}{45}\left(\frac{q^e}{p^e}\right)^2(h^e)^3\right] + q^e\left[\frac{1}{3}h^e - \frac{2}{45}\left(\frac{q^e}{p^e}\right)(h^e)^3 + \frac{2}{945}\left(\frac{q^e}{p^e}\right)^2(h^e)^5\right] \tag{17a}$$

$$A_{22}^e = A_{11}^e \tag{17b}$$

$$A_{12}^e = p^e\left[-\frac{1}{h^e}+\frac{7}{360}\left(\frac{q^e}{p^e}\right)^2(h^e)^3\right] + q^e\left[\frac{1}{6}h^e-\frac{7}{180}\left(\frac{q^e}{p^e}\right)(h^e)^3+\frac{31}{15120}\left(\frac{q^e}{p^e}\right)^2(h^e)^5\right] \quad (17c)$$

$$A_{21}^e = A_{12}^e \quad (17d)$$

$${}_aA_{11}^e = \frac{2}{945}\left(\frac{q^e}{p^e}\right)^2(h^e)^5 f(x_1^e) \quad (17e)$$

$${}_aA_{22}^e = \frac{2}{945}\left(\frac{q^e}{p^e}\right)^2(h^e)^5 f(x_2^e) \quad (17f)$$

$${}_aA_{12}^e = \frac{31}{15120}\left(\frac{q^e}{p^e}\right)^2(h^e)^5 f(x_2^e) \quad (17g)$$

$${}_aA_{21}^e = \frac{31}{15120}\left(\frac{q^e}{p^e}\right)^2(h^e)^5 f(x_1^e) \quad (17h)$$

In general cases, b_i^e needs to be evaluated numerically. Note that ${}_aA_{ij}^e$s are no longer necessarily symmetric. Formally, in the case of $(\frac{q^e}{p^e}) \to 0$, the algorithm reduces to the first order Lagrange interpolation. Although we can take out items with $(\frac{q^e}{p^e})$ factors, we cannot simply consider the first order Lagrange interpolation as a reduced case of the new PSFEM because $(\frac{q^e}{p^e})$ are not zero in general. Therefore, two completely different elements, not two versions of the same element, will be compared in the next section.

4. NUMERICAL EXAMPLES

It is very easy to implement the above algorithm. Its effects must be examined with typical examples. Several examples from electromagnetics are presented. All examples are not only typical but also analytically solvable. So, comparisons are reliable and stable. Some numerical error comparisons are provided in all examples. In most cases, except for the analytical solutions, the present element PSFEM is also compared with the first order Lagrange element. Although the PSFEM is inherently cubic element, they are still comparable since the PSFEM keeps the simplicity of the first order Lagrange element, most importantly the same bandwidth of the system matrices. Different examples are presented to illustrate effects on lossy, lossless, uniform, and nonuniform cases etc. The last example shows some comparison against the traditional cubic polynomials. In this paper, only uniform meshes are used. Because of the improvement on

hardware of computers, the 1D problem itself is no longer a challenge. To demonstrate the new element, only few elements are used to exaggerate the effects in simple examples.

4.1. A Simple Lossy Direct-Current Transmission Line

This example is used in [3] to illustrate FEM. The governing transmission line equations are

$$\frac{dv}{dx} = ri \tag{18a}$$

$$\frac{di}{dx} = gv \tag{18b}$$

where r and g are resistance per unit length and conductance per unit length respectively. Decoupling the above equations yields the second-order equation in voltage

$$\frac{d^2v}{dx^2} - rgv = 0 \tag{19}$$

Assume that there is a source V_0 at $x = 0$, the other end $x = L$ is open $i = 0$, then the boundary conditions of (19) are

$$v|_{x=0} = V_0 \tag{20a}$$

$$\left.\frac{dv}{dx}\right|_{x=L} = 0 \tag{20b}$$

(19) and (20) form the complete mathematical descriptions of the problem with analytical solution

$$v = V_0 \frac{e^{\sqrt{rg}(L-x)} + e^{-\sqrt{rg}(L-x)}}{e^{\sqrt{rg}L} + e^{-\sqrt{rg}L}} \tag{21}$$

The variational expression can be derived by considering the power loss per unit length as

$$W = -\int_0^L \left[\frac{1}{r}\left(\frac{dv}{dx}\right)^2 + gv^2\right] dx \tag{22}$$

This is identical to (4) in this case. As pointed out in [3], (22) represents a physics law and is not open to choice. This implies, from the physical point of view, Rayleigh-Ritz method is preferable whenever possible. We will discuss this point later.

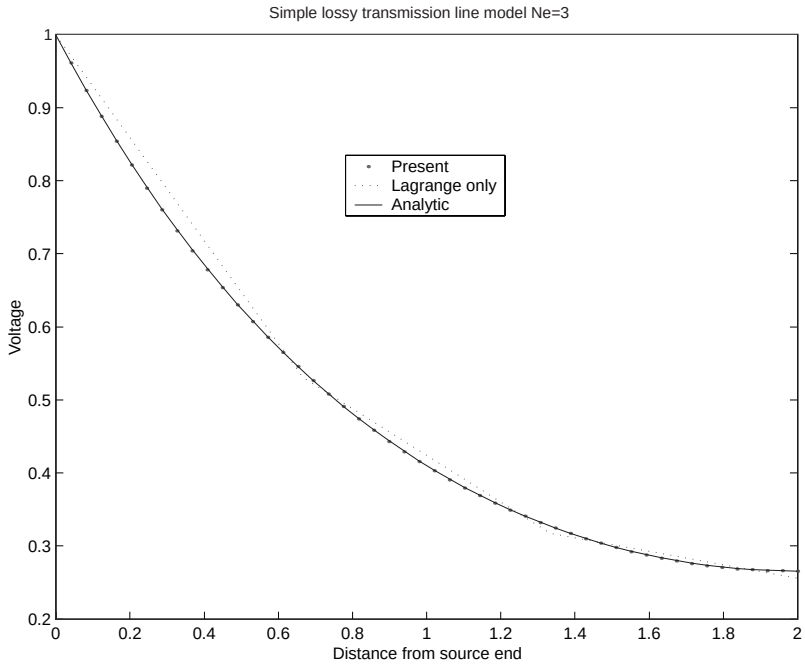

Figure 1. Voltage distribution of a simple lossy line.

Comparing the above equations with (1), (2) and (3), we have $p = -1$, $q = rg$ and $f = 0$, $Q = V$ at $x = 0$, $\alpha = 0$ and $\beta = 0$ at $x = L$. In order to compare with existing literature, we use the same numerical parameter as those used in [3]. Let $L = 1$, $V = 1$, and $\sqrt{rg} = 1$. The numerical solutions of the first order Lagrange interpolation are compared with the results of (21) in Fig. 1. The number of element $Ne = 3$. Note that the physical spline interpolation (8) should be used to interpolate the values between two adjacent nodes. Instead, it is a straight line between two nodes in the Lagrange interpolation. The maximum relative error of the present method is 0.27%, but is 1.85% in the Lagrange interpolation algorithm. A great improvement is seen. As we expect that the smoothness is also much better than the Lagrange interpolation.

Table 1. Comparison of three methods for the fields between two plates.

Node#	E_y			Absolute error	
	Analytical	Present	Lagrange	Present	Lagrange
1	0	0	0	0	0
2	0.309016994	0.309016869	0.310286676	−0.000000125	0.001269681
3	0.587785252	0.587785013	0.590200330	−0.000000239	0.002415077
4	0.809016994	0.809016666	0.812341063	−0.000000329	0.003324068
5	0.951056516	0.951056130	0.954964193	−0.000000386	0.003907677
6	1.000000000	0.999999594	1.004108775	−0.000000406	0.004108775
7	0.951056516	0.951056130	0.954964193	−0.000000386	0.003907677
8	0.809016994	0.809016666	0.812341063	−0.000000329	0.003324069
9	0.587785252	0.587785014	0.590200330	−0.000000239	0.002415077
10	0.309016994	0.309016869	0.310286676	−0.000000125	0.001269681
11	0	0	0	0	0

4.2. Wave between Parallel Plates

This example is solved using FEM in [5]. The differential equation and boundary conditions are

$$-\frac{d^2E_y(x)}{dx^2} + \pi^2 E_y(x) = 2\pi^2 \sin(\pi x), \quad (0 \le x \le 1) \tag{23a}$$

$$E_y(0) = E_y(1) = 0 \tag{23b}$$

Its exact solution is

$$E_y(x) = \sin(\pi x) \tag{24}$$

Obviously

$$p(x) = 1, \quad q(x) = \pi^2, \quad f(x) = 2\pi^2 \sin(\pi x) \tag{25}$$

In order to ensure the reliability of our comparison, all integrals of b_i^e are also performed analytically in our computations. The same number of nodes $N = 11$ used in [5] is used. Table 1 compares our results and the existing numerical results (Lagrange interpolation) with the exact solutions in details. Because the error of our results is so small that long format is displayed.

As seen, the accuracy of our results is in the seventh decimal place, instead of in the third decimal place given in [5]. Obviously, this is really impressive. To emphasize the dramatic improvement, Fig. 2 compares the corresponding results when the number of nodes $N = 4$. Even in this extreme case, the present results are satisfactory, the results of Lagrange interpolation are too bad.

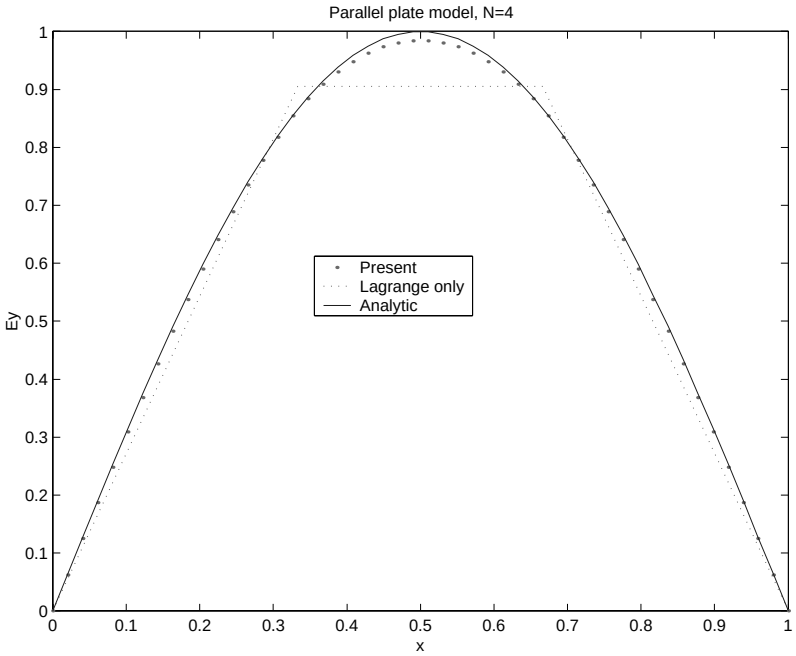

Figure 2. Fields between parallel plates.

4.3. Reflection from a Grounded Dielectric Slab at Normal Incidence

This problem is described by the differential equation and boundary conditions for E_z-polarized wave

$$\frac{d^2E_z}{dx^2} + k_0^2\epsilon_r E_z = 0 \tag{26a}$$

$$E_z(0) = 0 \tag{26b}$$

$$\frac{\partial E_z}{\partial x} + jk_0 E_z = 2jk_0 e^{jk_0 x} \tag{26c}$$

The same configuration used in [5] is used here. The thickness $t = 0.25$, $\mu_r = 1$ and $\epsilon_r = 4 - j\beta$. $x_a = t + \Delta t$. The analytical reflection coefficient is given by

$$R = -\frac{Z_0 - jZ\tan(k_0\sqrt{\epsilon_r}t)}{Z_0 + jZ\tan(k_0\sqrt{\epsilon_r}t)} \tag{27}$$

where $Z_0 = 120\pi$ and $Z = Z_0/\sqrt{\epsilon_r}$. From (26), $p = -1,\ q = k_0^2\epsilon_r,\ \alpha =$

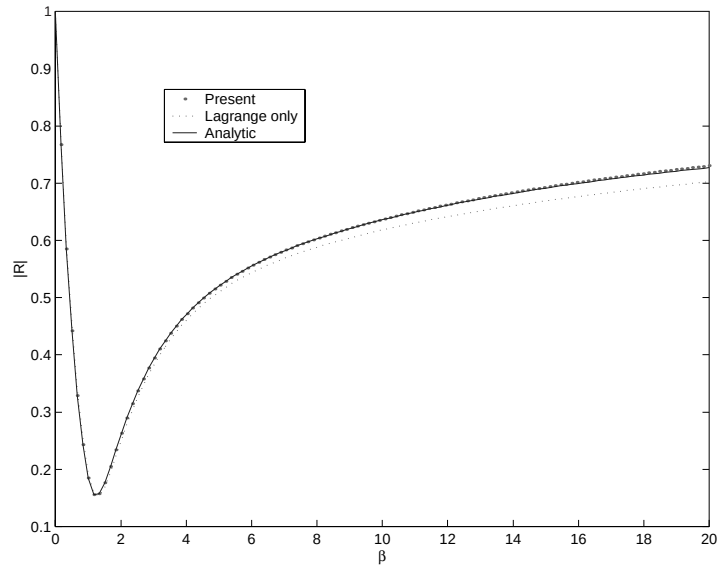

Figure 3. Reflection (normal incidence) versus β from a grounded dielectric slab with $t = 0.25\lambda_0,\ \epsilon = 4 - j\beta,\ N = 6$.

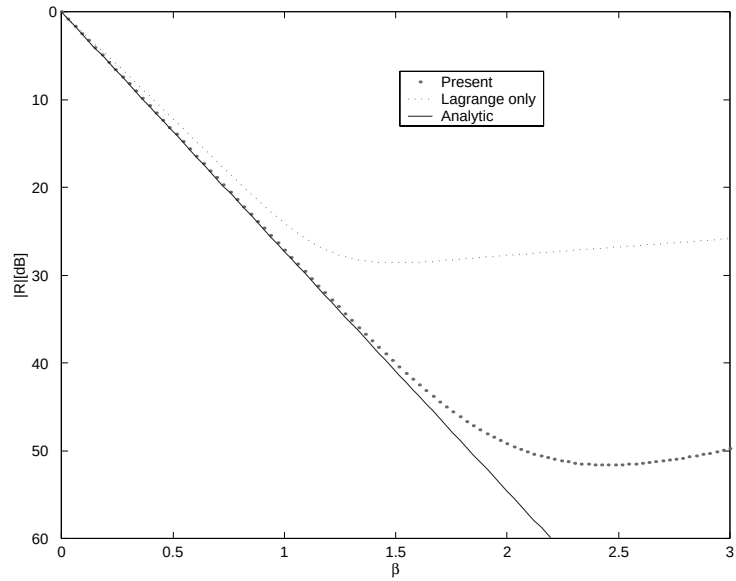

Figure 4. Reflection (normal incidence) versus β from a grounded dielectric slab with $t = 0.25\lambda_0,\ \epsilon = \mu_r = 4 - j\beta,\ N = 7$.

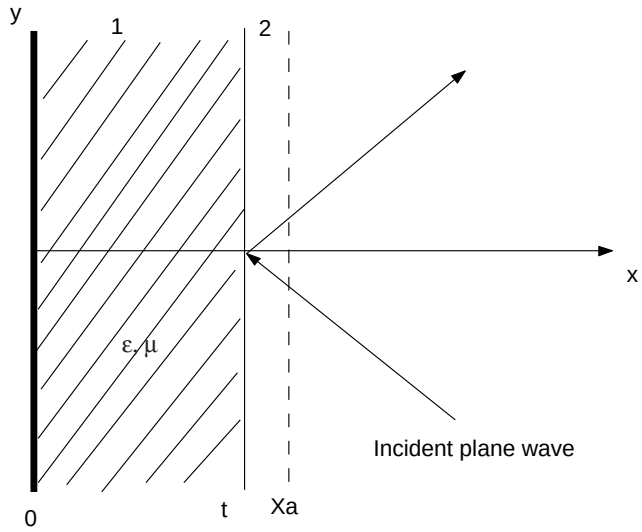

Figure 5. Planar absorbing layer analysis.

jk_0 and $\beta = 2jk_0e^{jk_0x_a}$.

The results of the present PSFEM, the Lagrange interpolation and analytic method are compared in Fig. 3. The number of nodes $N = 6$. The number of elements in the slab is 4 and 1 layer is in the air. It is noticed that the physical spline results are in a very good agreement with analytical solutions even for very high lossy slabs.

The following examples are also scattering problems.

4.4. Reflectionless Slab-E_z Polarized and Normal Incidence

This example is used to illustrate the powerful effects of the PSFEM. We will discuss a more general case in the next section. All parameters are the same as in Example 3 except for $\epsilon_r = \mu_r = 4 - j\beta$. So the discontinuity is serious at the interface. The exact solution to the reflection is $R = -e^{-2jk_0\epsilon_r t}$. Fig. 4 shows the comparison when the number of elements in the slab $N = 7$, which implies the number of elements in the slab is 5. Comparable results for other number of layers using Lagrange interpolation are found in [5] Fig. 3.12. It is easy to conclude that the PSFEM results with $N = 7$ are much better than the existing FEM results. They are better than the Lagrange results with $N = 12$.

4.5. Design of Planar Absorbing Layers

4.5.1. Problem Description and Equations

Let us discuss a more general case of Example 4 — the design of planar absorbing layers. This problem has important applications in FEM simulations. Error analysis will be given numerically.

As illustrated in Fig. 5, an arbitrarily polarized plane wave incidents on the metal-backed slab. The Ez polarized component is

$$E_z^{inc}(x,y) = E_0 e^{jk_0 x\cos\phi - jk_0 y\sin\phi} \tag{28}$$

and Hz-polarized component

$$H_z^{inc}(x,y) = H_0 e^{jk_0 x\cos\phi - jk_0 y\sin\phi} \tag{29}$$

In our implementation of FEM, one air layer at $x = x_a$ is added to truncate the solution region.

As discussed in [4], the wave equations that govern the total fields between $x = 0$ and $x = x_a$ and the corresponding boundary conditions can be summarized as follows

1. Ez-polarized

$$\frac{d}{dx}\left(\frac{1}{\mu_r}\frac{E_z}{dx}\right) + k_0^2\left(\epsilon_r - \frac{1}{\mu_r}\sin^2\phi\right)E_z = 0 \tag{30a}$$

$$E_z\Big|_{x=0} = 0 \tag{30b}$$

$$\left[\frac{dE_z}{dx} + jk_0\cos\phi E_z\right]\Big|_{x=x_a} = 2jk_0\cos\phi E_0 e^{jk_0 x_a\cos\phi} \tag{30c}$$

2. Hz-polarized

$$\frac{d}{dx}\left(\frac{1}{\epsilon_r}\frac{H_z}{dx}\right) + k_0^2\left(\mu_r - \frac{1}{\epsilon_r}\sin^2\phi\right)H_z = 0 \tag{31a}$$

$$\frac{dH_z}{dx}\Big|_{x=0} = 0 \tag{31b}$$

$$\left[\frac{dH_z}{dx} + jk_0\cos\phi H_z\right]\Big|_{x=x_a} = 2jk_0\cos\phi H_0 e^{jk_0 x_a\cos\phi} \tag{31c}$$

We do not need to enforce the inner boundary conditions at $x = t$.

4.5.2. Analytical Solution — Reflection

The closed forms are found in [18]. In order to compare, we list the results with corrections,

$$R_E(\phi) = -\frac{a - j\cos\phi\tan(k_0 abt)}{a + j\cos\phi\tan(k_0 abt)} \tag{32}$$

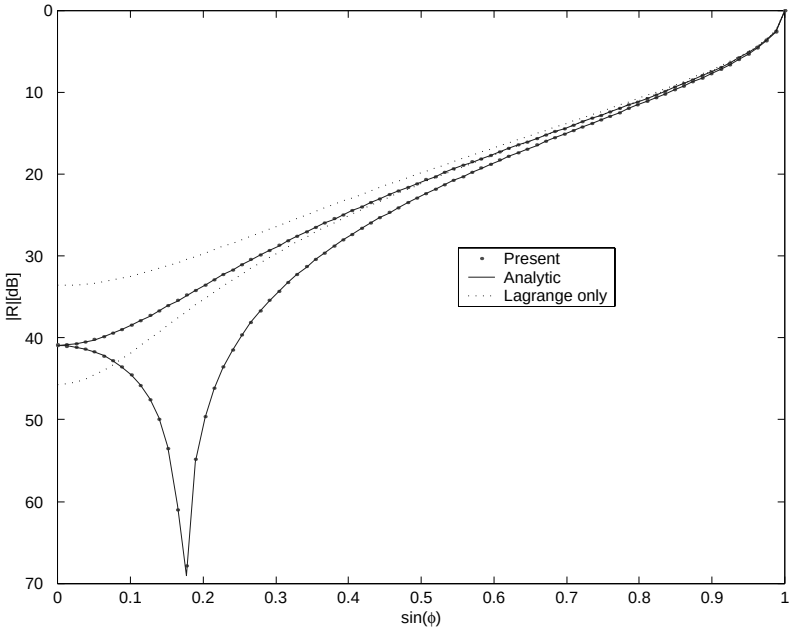

Figure 6. Reflected by metal-backed layers. $N = 5$, upper-E_z, lower-H_z.

$$R_H(\phi) = -\frac{a + j\cos\phi\cot(k_0 abt)}{a - j\cos\phi\cot(k_0 abt)} \tag{33}$$

where $b = \epsilon_r = \mu_r = \alpha - j\beta$ and $a = \sqrt{1 - (\sin\phi/b)^2}$. Of course, the α and β are not those in (3).

4.5.3. Reflection Comparison

It is quite straightforward to perform FEM analysis by comparing (30) and (31) with (1), (2) and (3). Some typical results are plotted in Fig. 6. The number of nodes $N = 5$, which indicates that there are three layers in the slab. $t = 0.15$ and $b = -j2.5$ are used, then it is easy to verify our computation with [18]. Not surprisingly, the PSFEM results are in very good agreements with the analytical ones. In contrary to this, the Lagrange results are not acceptable. As seen in Figure 3 of [18], the Lagrange method cannot obtain the same accuracy even with twelve layers in the slab ($N = 14$ in our case). It is known that modeling rapidly decaying fields is not easy. But the PSFEM works well.

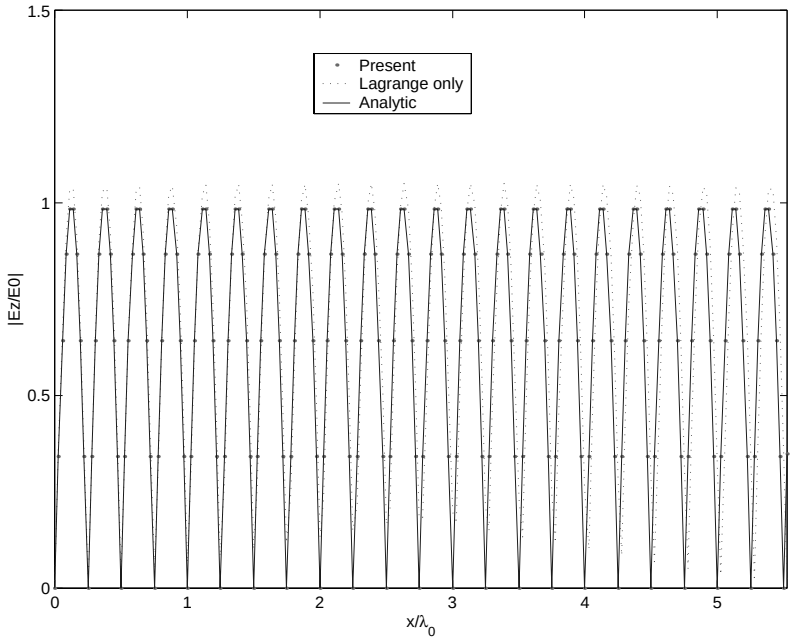

Figure 7. Reflected by metal-backed layers. Amplitude, $N = 200$.

4.5.4. Field Comparison

Although the reflection coefficient of a metal-backed slab is important, the fields in the region give us insight information. Checking the fields helps us understand the details of various algorithms and perform error analysis, then finally evaluate algorithms. Let us consider normal incidence Ez-polarized case only. According to [22, p. 52] and [4, p. 50], the fields in the slab (region 1 in Fig. 5) are given by

$$E_{z1}(x) = \frac{E_{z2}(t)}{\sin(k_0\sqrt{\epsilon_r\mu_r}t)}\sin(k_0\sqrt{\epsilon_r\mu_r}x) \tag{34}$$

$$E_{z2}(x) = e^{jk_0x} + R_2e^{-jk_0x} \tag{35}$$

where

$$R_2 = \frac{\eta_{2,1} - e^{-2jk_0\sqrt{\epsilon_r\mu_r}t)}}{1 - \eta_{2,1}e^{-2jk_0\sqrt{\epsilon_r\mu_r}t)}}e^{2jk_0t} \tag{36}$$

$$\eta_{2,1} = \frac{\sqrt{\mu_r} - \sqrt{\epsilon_r}}{\sqrt{\mu_r} + \sqrt{\epsilon_r}} \tag{37}$$

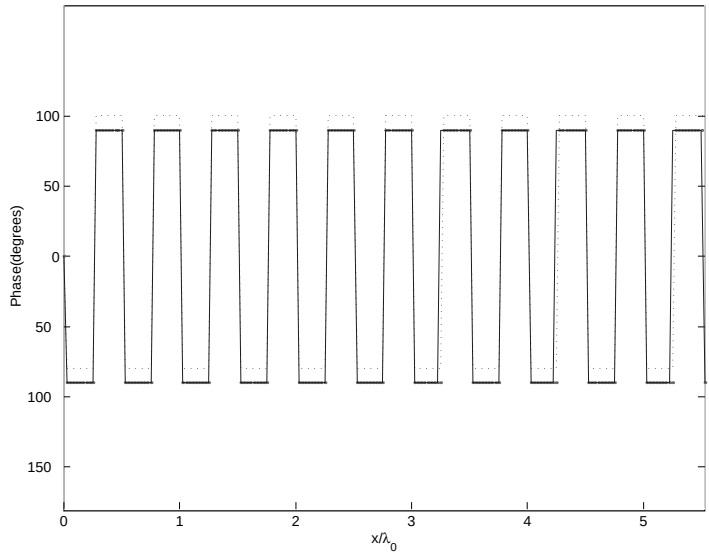

Figure 8. Reflected by metal-backed layers. Phase, $N = 200$.

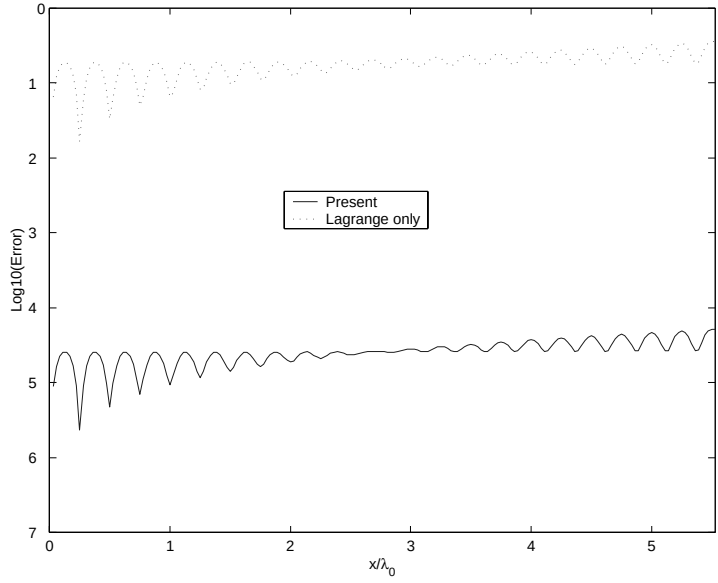

Figure 9. Reflected by metal-backed layers. Error, $N = 200$, $t/\lambda_0 = 5.5$.

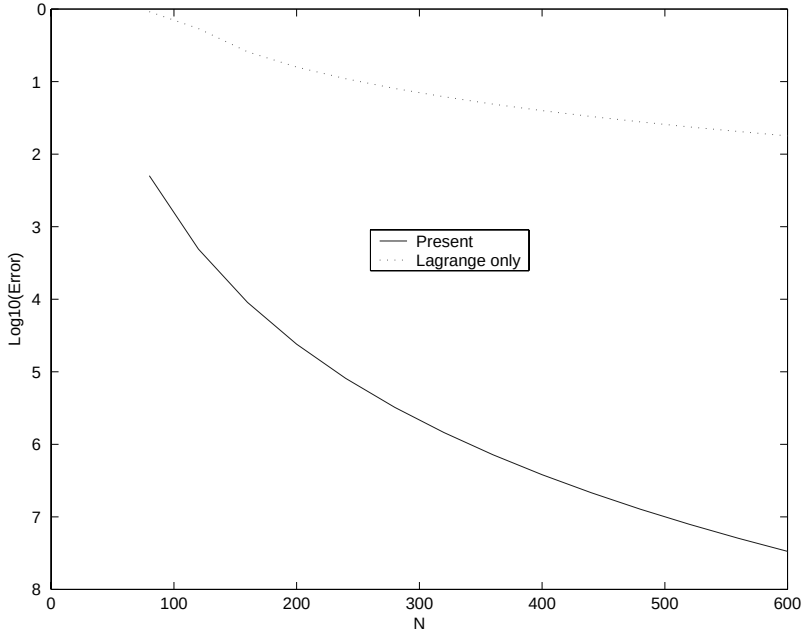

Figure 10. Reflected by metal-backed layers. Average error versus $N,\ t/\lambda_0 = 5.5$.

Let $\epsilon_r = 4,\ \mu_r = 1$ and $t = 5.5\lambda_0,\ N = 200$. Fig. 7 compares the amplitude of fields, Fig. 8 the corresponding phases. The same legends apply. Again, the PSFEM results are very good. It is worthy of taking a look at Fig. 9 and Fig. 10. They are quantitative error analysis and comparable with Figure 3.15 and Figure 3.16 of [4]. Fig. 9 is the error along x axis. It shows that the PSFEM is much better than the first order Lagrange algorithm. Furthermore, comparing Fig. 9 and Fig. 10 with Figure 3.15 and Figure 3.16 in [4], we can see that the physical spline field computation is even much better than the cubic Lagrange computation. We know that the implementation of higher-order (cubic or higher) Lagrange interpolations is very complicated, usually results in complex formulation, increases the bandwidth of the system equations and then increases the computing time. Increasing the number of nodes improves the accuracy rapidly as shown in Fig. 10. Fig. 10 is a plot of the average error versus the number of nodes.

5. CONCLUDING REMARKS

In this paper, a new technique — physical spline finite element method (PSFEM) — is first developed. In this technique, physical differential equations are first incorporated into interpolations of basic elements in FEM. Its effects are verified by several typical examples from 1D electromagnetic problems. Theoretically, the PSFEM introduces many new features. First, as we mentioned, physical equations can be used in the interpolation. This makes the interpolation problem-associated. The algorithm must converge much faster than general interpolations. The simplicity of the first order Lagrange interpolation is remained. The corresponding implementation is different from traditional splines such as B-splines. Second, the concept of basis functions may need to be re-examined. It is not easy to point out the basis functions in (8) and (9) since the second term has nothing to do with the unknown U or its derivatives. From this point of view, Rayleigh-Ritz's formulation is better than Galerkin's formulation. We are not confused by the choice of weighted functions from (8) or (9). Also, as pointed out in the first example, the corresponding formation is not open to choice because of its physics considerations. Unfortunately, not all problems can be formulated via the Rayleigh-Ritz's method. The application of the new element in the Galerkin's method needs to be investigated. Thirdly, if we still name $B_i^e(x)$s defined by (10) as basis functions, they could be complex without intuitive and simple geometric explanations. They are no longer always real as claimed in [4]. Finally, the PSFEM limits the solutions within the physical solution space, which is $C^2[0,1]$ in this case.

We may argue that the new element is cubic. This is true. However, it is not just simple cubic. It is based on the cubic spline and physical equations. The same simplicity with the first order Lagrange interpolation makes our comparisons in the examples meaningful. More comparisons against higher order (p- and hp-) elements will be an interesting topic even though higher order elements have inherent smoothness problems as discussed in the introduction.

Obviously, more theoretical investigations on the newly developed technique are needed. On the other hand, it should be applied to more applications and extended to two-and three-dimensional problems. In principle, the extension of a 1D interpolation to higher dimension is possible as described in [20]. However, we may face some other challenges in our case. One way of the extension to two-dimensional problems is described in [23]. Its application to waveguide problems is presented in [24]. Its extension to 3D problems is still under investigation.

This paper presents and emphasizes the basic idea rather than specific examples. The concept is applicable to other disciplines and other numerical methods.

ACKNOWLEDGMENT

The author would like to express thanks to Dr. George Pan at Arizona State University for allowing him to work freely and Dr. Weigan Lin at University of Electronic Science and Technology of China for encouragement in his research career.

REFERENCES

1. Zienkiewicz, O. C., *The Finite Element Method in Structural and Continuum Mechanics*, McGraw-Hill, New York, 1967.
2. Kwon, Y. W. and H. Bang, *The Finite Element Method Using MATLAB*, CRC Press, Boca Raton, 1997.
3. Silvester, P. P., *Finite Elements for Electrical Engineers*, Cambridge University Press, New York, 1996.
4. Jin, J., *The Finite Element Method in Electromagnetics*, John Wiley & Sons, New York, 1993.
5. Volakis, J. L., A. Chatterjee, and L. C. Kempel, *Finite Element Method for Electromagnetics: Antennas, Microwave Circuits, and Scattering Applications*, IEEE Press, New York, 1998.
6. Silvester, P. P. and G. Pelosi, *Finite Elements for Wave Electromagnetics: Method and Techniques*, IEEE Press, New York, 1994.
7. Babuska, I. and M. Suri, "The p and hp versions of the finite element methods, basic principles and properties," *SIAM Rev.*, Vol. 36, 578–632, 1994.
8. Melenk, J., K. Gerdes, and C. Schwab, "Fully discrete hp-finite elements: fast quadrature," *Compu. Methods Appli. Mech. Engrg.*, Vol. 190, 4339–4364, October 2001.
9. Noor, A. K. and W. D. Pilkey, *State-of the Art Surveys on Finite Element Technology*, American Society of Mechanical Engineers, New York, 1983.
10. Cheney, W. and D. Kincaid, *Numerical Mathematics and Computing*, Brooks/Cole Publishing Company, Pacific Grove, 1994.
11. Castillo, L. E. G., T. K. Sarkar, and M. S. Palma, "An efficient finite element method employing wavelet type basis functions

(waveguide analysis)," *COMPEL — The International Journal for Computation and Mathematics in Electrical and Electronic Engineering*, Vol. 13, 278–292, May 1994.

12. Mitchell, A. R., "Variational principles and the finite element method," *J. Inst. Maths. Applications*, Vol. 9, 378–389, 1972.
13. Benjeddou, A., "Vibrations of complex shells of revolution using B-spline finite elements," *Computer & Structures*, Vol. 74, 429–440, April 2000.
14. Ahlberg, J. H., E. N. Nilson, and J. L. Walsh, *The Theory of Splines and Their Applications*, Academic Press, New York, 1967.
15. Prenter, P. M., *Splines and Variational Methods*, Wiley, New York, 1975.
16. de Boor, C., *A Practical Guide to Spline*, Springer-Verlag, New York, 1978.
17. Liang, X., B. Jian, and G. Ni, "The B-spline finite element method in electromagnetic field numerical analysis," *IEEE Trans. on Magnetics*, Vol. MAG-23, 2641–2643, Sept. 1987.
18. Legault, S. R., T. B. A. Senior, and J. L. Volakis, "Design of planar absorbing layers for domain truncation in FEM applications," *Electromagnetics*, Vol. 16, 451–464, July 1996.
19. Liang, X., B. Jian, and G. Ni, "B-spline finite element method applied to axi-symmetrical and nonlinear field problems," *IEEE Trans. on Magnetics*, Vol. 24, 27–30, Jan. 1988.
20. Press, W. H. and S. A. Tewkdsky, *Numerical Recipes in C, The Art of Scientific Computing*, Cambridge University Press, New York, 1992.
21. Allen, M. B. and E. L. Isaacson, *Numerical Analysis for Applied Science*, Wiley, 1997.
22. Chew, W. C., *Waves and Fields in Inhomogeneous Media*, Van Nostrand Teinhold, New York, 1990.
23. Zhou, X., "Physical spline finite element method in microwave engineering," Ph.D. thesis, Arizona State University, May 2001.
24. Zhou, X. and G. Pan, "Application of physical spline FEM to waveguide problems," *PIERS 2000 Progress in Electromagnetics Research Symposium*, 77, Boston, USA, July 2002.